Draft for Preliminary Writeup, March 20, 2019

HERAPDF2.0Jets NNLO (prel.), the completion of the HERAPDF2.0 family

H1, ZEUS and NNLOJET Collaborations

Abstract

The HERAPDF2.0 family, introduced in 2015, is completed with fits HERAPDF2.0Jets NNLO (prel.) based on inclusive HERA data and selected jet production data. A fit with a free strong coupling constant, $\alpha_s(M_Z^2)$, gave $\alpha_s(M_Z^2) = 0.1150 \pm 0.0008(\mathrm{exp})^{+0.0002}_{-0.0005}(\mathrm{model/parameterisation}) \pm 0.0006(\mathrm{hadronisation}) \pm 0.0027(\mathrm{scale})$. Sets of parton density functions, PDFs, from fits with fixed $\alpha_s(M_Z^2) = 0.115$ and $\alpha_s(M_Z^2) = 0.118$ are presented and compared. The PDFs from the fit with fixed $\alpha_s(M_Z^2) = 0.118$ are also compared to the PDFs from HERAPDF2.0 NNLO. Predictions from the PDFs of HERAPDF2.0Jets NNLO (prel.) with fixed $\alpha_s(M_Z^2) = 0.115$ are compared to the jet production data used as input. The prediction describe the data very well.

1 Introduction

Deep inelastic scattering (DIS) of electrons on protons, ep, at centre-of-mass energies of up to $\sqrt{s} \simeq 320\,\text{GeV}$ at HERA has been central to the exploration of proton structure and quark–gluon dynamics as described by perturbative Quantum Chromo Dynamics (pQCD) [1].

The combination of H1 and ZEUS data on inclusive ep scattering and the subsequent pQCD analysis, introducing of the family of parton density functions (PDFs) known as HERAPDF2.0, was a milestone for the exploitation[2] of the HERA data. The preliminary work presented here represents a completion of the HERAPDF2.0 family [2] with a fit at NNLO to inclusive and jet production data published separately by the ZEUS and H1 collaborations. This was not possible at the time of the original introduction of HERAPDF2.0 because a treatment at NNLO of jet production in deep inelastic ep scattering was not available then.

The name HERAPDF stands for a pQCD analysis within the DGLAP [3–7] formalism, where predictions from pQCD were fitted to data. These predictions were obtained by solving the DGLAP evolution equations at LO, NLO and NNLO in the $\overline{\text{MS}}$ scheme [8].

2 Procedure and Data

The inclusive and dijet production data [9–13], which were already used for HERAPDF2.0Jets NLO were again used for the analysis presented here. A new data set [14] on jet production in low Q^2 events, where Q^2 is the four-momentum-transfer squared, was added as input to the fits. All data sets on jet production are listed in Table 1. The analysis presented here does not include the charm data which were included in the analysis at NLO. Their influence will be studied in a future analysis.

The fits presented here were done in almost exactly the same way [2] as for all other members of the HERAPDF2.0 family [2], and especially for the HERAPDF2.0Jets NLO fit. The fits were performed using the programme QCDNUM [15] within the xFitter, formerly HERAFitter, framework [16] and an independent programme, which was also already used as a second program in the HERAPDF2.0 analysis. The results obtained by the two programmes, as previously for all HERAPDF2.0 fits [2], were in excellent agreement, well within fit uncertainties. All numbers presented here were obtained using xFitter. Only cross sections for Q^2 starting at $Q^2_{min} = 3.5\,\text{GeV}^2$ were used in the analysis. All parameter setting were the same as for the HERAPDF2.0Jets NLO fit. The analysis of uncertainties was also performed in exactly the same way.

The modification of the procedure was driven by the usage of the newly available treatment of jet production at NNLO. The jet data were included in the fits at NNLO by calculating predictions for the jet cross sections within the Applfast framework using NLOjet++ [17,18], which was interfaced to FastNLO [19–21] in order to achieve the speed necessary for iterative PDF fits. The predictions were multiplied by corrections for hadronisation and Z^0 exchange before they were used in the fits. A running electro-magnetic α as implemented in the 2012 version of the programme EPRC [22] was used for the treatment of the jet cross sections.

The treatment of inclusive jet and dijet production at NNLO was only applicable to a slightly reduced phase space compared to HERAPDF2.0Jets NLO. All data points with $\sqrt{\langle p_T^2 \rangle + Q^2} \leq$

13.5 GeV were excluded, where p_T is the transverse energy of the jets. In addition, six data points, the lowest $\langle p_T \rangle$ bin for each Q^2 region, were excluded from the ZEUS dijet data set because the NNLO predictions for these points were deemed unreliable. The resulting reduction of data points is given in Table 1. In addition, the trijet data [13] which were used as input to HERAPDF2.0Jets NLO had to be excluded as their treatment at NNLO was not available.

The choice of scales was also adjusted to the NNLO analysis. At NLO, the factorisation scale was chosen as $\mu_{\rm f}^2 = Q^2$, while the renormalisation scale was linked to the transverse momenta, p_T, of the jets by $\mu_{\rm r}^2 = (Q^2 + p_T^2)/2$. For the NNLO analysis, $\mu_{\rm f}^2 = \mu_{\rm r}^2 = Q^2 + p_T^2$ was chosen.

3 Determination of the strong coupling constant

The jet production data are essential for the determination of the strong coupling constant, $\alpha_s(M_Z^2)$. In pQCD fits to inclusive DIS data alone, the gluon PDF is determined via the DGLAP equations using the observed scaling violations. This results in a strong correlation between the shape of the gluon distribution and the value of $\alpha_s(M_Z^2)$. Data on jet production cross sections provide an independent constraint on the gluon distribution. Jet production is also directly sensitive to $\alpha_s(M_Z^2)$ and thus allows for an accurate simultaneous determination of $\alpha_s(M_Z^2)$ and the gluon distribution.

The HERAPDF2.0Jets NNLO (prel.) fit with free $\alpha_s(M_Z^2)$ gave a value of

$$\begin{aligned}\alpha_s(M_Z^2) = 0.1150 \pm 0.0008(\text{exp})^{+0.0002}_{-0.0005}(\text{model/parameterisation})\\ \pm 0.0006(\text{hadronisation}) \quad \pm 0.0027(\text{scale}) \;.\end{aligned}$$

This result on $\alpha_s(M_Z^2)$ is compatible with the world average [23] and it is competitive with other determinations at NNLO.

The χ^2/d.o.f. of this HERAPDF2.0Jets NNLO (prel.) fit uses 1343 data points and has a $\chi^2/\text{d.o.f.} = 1599/1328 = 1.203$. This can be compared to the $\chi^2/\text{d.o.f.} = 1363/1131 = 1.205$ for HERAPDF2.0 NNLO based on inclusive data only. This indicates that there is no tension introduced by the data on jet production.

The experimental uncertainty was determined from the fit. The χ^2 scan in $\alpha_s(M_Z^2)$ shown in Fig. 1a) confirmed the value of $\alpha_s(M_Z^2)$ and the experimental, i.e. fit, uncertainty. The clear minimum coincides with the value as determined by the fit and the dependence of χ^2 on $\alpha_s(M_Z^2)$ confirms the fit uncertainty. The model/parameterisation and hadronisation uncertainties were determined with similar scans in the respective parameter space.

A strong motivation to determine $\alpha_s(M_Z^2)$ at NNLO was the hope to substantially reduce scale uncertainties. This uncertainty was evaluated by varying the renormalisation and factorisation scales by a factor of two, both separately and simultaneously, and taking the maximal positive and negative deviations. The uncertainties were assumed to be 50 % correlated and 50 % uncorrelated between bins and data sets.

As the input data were changed for the NNLO analysis and the choice of scales were changed with respect to the NLO analysis, a detailed comparison will be published after an appropriate reanalysis of the data at NLO. However, the scale uncertainty of ±0.0027) is significantly lower than the +0.0037, −0.0030. previously observed for the HERAPDF2.0Jets NLO analysis. If the NNLO determination of $\alpha_s(M_Z^2)$ was performed with the old choice of scales, the value of $\alpha_s(M_Z^2)$ was reduced to 0.1135. This is well within scale uncertainties.

The question whether data with relatively low Q^2 bias the determination of $\alpha_s(M_Z^2)$ arose within the context of the HERAPDF2.0 analysis [2]. Figure 1b) shows scans with Q^2_{min} set to 3.5 GeV^2, 10 GeV^2 and 20 GeV^2 for the inclusive data. Clear minima are visible which coincide within uncertainties.

4 The PDFs of HERAPDF2.0Jets NNLO (prel.)

The PDFs resulting from the HERAPDF2.0Jets NNLO (prel.) fit with $\alpha_s(M_Z^2) = 0.115$ are shown in Fig. 2 at a scale of $Q^2 = 10\,\text{GeV}^2$. The results of a full analysis of uncertainties obtained from the respective fits are also shown. This includes experimental uncertainties, model and parameterisation uncertainties as well as additional hadronisation uncertainties on the jet data, all as defined for the HERAPDF2.0 family [2].

The PDFs resulting from the HERAPDF2.0Jets NNLO (prel.) fit with $\alpha_s(M_Z^2) = 0.118$, the value used for HERAPDF2.0Jets NLO, are shown in Fig. 3 at a scale of $Q^2 = 10\,\text{GeV}^2$. Also shown are the results of a full analysis of uncertainties. A comparison between the PDFs obtained for $\alpha_s(M_Z^2) = 0.115$ and $\alpha_s(M_Z^2) = 0.118$ is shown in Fig. 4. Here, only total uncertainties are shown. A significant difference is only observed in the gluon distributions, where the distribution for $\alpha_s(M_Z^2) = 0.115$ is above the distribution for $\alpha_s(M_Z^2) = 0.115$ for x less than $\approx 10^{-2}$.

A comparison between the PDFs obtained by HERAPDF2.0Jets NNLO (prel.) with $\alpha_s(M_Z^2) = 0.118$ and the PDFs of HERAPDF2.0 NNLO based on inclusive data only is shown in Fig. 5. Again, only total uncertainties are shown. These two sets of PDFs do not show any significant difference.

5 Comparison of HERAPDF2.0Jets NNLO (prel.) to jet data

Comparisons of the predictions of HERAPDF2.0Jets NNLO (prel.) to the data on jet production used as input are shown in Figs. 6, 7, 8 and 9. The H1 collaboration published most of their jet cross sections normalised to the inclusive NC cross sections.

All analyses were performed using the assumption of massless jets, i.e. the transverse energy, E_T, and the transverse momentum of a jet, p_T, are equivalent. For inclusive jet analyses, each jet is entered separately with its p_T. For dijet analyses, the average of the transverse momenta is used as p_T. These different definitions of p_T were also used to set the the factorisation and renormalisation scales to $\mu_\mathrm{f}^2 = \mu_\mathrm{r}^2 = Q^2 + p_T^2$ for calculating predictions. Scale uncertainties were not considered for the comparisons to data.

The predictions from HERAPDF2.0Jets NNLO (prel.) agree very well with all data on jet production used as input to the fit.

6 Summary

The HERA data set on inclusive *ep* scattering as introduced by the ZEUS and H1 collaborations [2], together with selected data on jet production, published separately by the two collaborations, were used as input to NNLO fits called HERAPDF2.0Jets NNLO (prel.). They complete the HERAPDF2.0 family. A fit with free $\alpha_s(M_Z^2)$ gave $\alpha_s(M_Z^2) = 0.1150 \pm 0.0008(\text{exp})^{+0.0002}_{-0.0005}$(model/parameterisation) $\pm$ 0.0006(hadronisation) $\pm$ 0.0027(scale). A preliminary set of PDFs with a full analysis of uncertainties was obtained from a HERAPDF2.0Jets NNLO fit with fixed $\alpha_s(M_Z^2) = 0.115$. These PDFs were compared to PDFs from a similar fit with fixed $\alpha_s(M_Z^2) = 0.118$ and the PDFs from HERAPDF2.0 NNLO based on inclusive data only.

References

[1] A. Cooper-Sarkar and R. Devenish, *Deep inelastic Scattering*, Oxford Univ. Press (2011), ISBN 978-0-19-960225-4.

[2] H. Abramovicz *et al.* [ZEUS and H1 Collaboration], Eur. Phys. J. C **75**, 580 (2015), [arXiv:1506.06042].

[3] V. N. Gribov and L. N. Lipatov, Sov. J. Nucl. Phys. **15**, 438 (1972).

[4] V. N. Gribov and L. N. Lipatov, Sov. J. Nucl. Phys. **15**, 675 (1972).

[5] L. N. Lipatov, Sov. J. Nucl. Phys. **20**, 94 (1975).

[6] Y. L. Dokshitzer, Sov. Phys. JETP **46**, 641 (1977).

[7] G. Altarelli and G. Parisi, Nucl. Phys. B **126**, 298 (1977).

[8] B. Fanchiotti, S. Kniehl and A. Sirlin, Phys. Rev. D **48**, 307 (1993), [hep-ph/9803393].

[9] S. Chekanov *et al.* [ZEUS Collaboration], Phys. Lett. B **547**, 164 (2002), [hep-ex/0208037].

[10] H. Abramowicz *et al.* [ZEUS Collaboration], Eur. Phys. J. C **70**, 965 (2010), [arXiv:1010.6167].

[11] A. Aktas *et al.* [H1 Collaboration], Phys. Lett. B **653**, 134 (2007), [arXiv:0706.3722].

[12] F. Aaron *et al.* [H1 Collaboration], Eur. Phys. J. C **67**, 1 (2010), [arXiv:0911.5678].

[13] V. Andreev *et al.* [H1 Collaboration], Eur. Phys. J. C **65**, 2 (2015), [arXiv:1406.4709].

[14] V. Andreev *et al.* [H1 Collaboration], Eur. Phys. J. C **77**, 215 (2017), [arXiv:1611.03421].

[15] M. Botje, Comp. Phys. Comm. **182**, 490 (2011), [arXiv:1005.1481].

[16] S. Alekhin *et al.* (2014), [arXiv:1410.4412].

[17] Z. Nagy and Z. Trocsany, Phys. Rev. D **59**, 014020 (1999), [hep-ph/9806317].

[18] Z. Nagy, Phys. Rev. Lett. **88**, 122003 (2002), [hep-ph/0110315].

[19] C. Adloff *et al.*, Eur. Phys. J. C **19**, 289 (2001), [hep-ph/0010054].

[20] T. Kluge *et al.*, in *Proc. of 14th International Workshop on Deep Inelastic Scattering (DIS 2006)*, edited by M. Kuze, K. Nagano and K. Tokushuku (2007), p. 483, [hep-ph/0609285].

[21] D. Britzger *et al.*, in *Proc. of 20th International Workshop on Deep Inelastic Scattering and Related Subjects (DIS 2012)*, edited by I. Brock (2013), p. 217, [arXiv:1208.3641].

[22] H. Spiesberger, in *Proc. of Future Physics at HERA*, edited by G. Ingelman, A. De Roeck and R. Klanner (1995), p. 227.

[23] M. Tanabashi *et al.* (Particle Data Group), Phys. Rev. D **98**, 030001 (2018).

Data Set	published	Q^2[GeV^2] range from	to	$\mathcal{L}$ pb^{-1}	e^+/e^-	$\sqrt{s}$ GeV	norma-lised	all points	used points	Ref.
H1 high Q^2 HERA I incl. jets	2007	150	15000	65.4	e^+p	301	yes	24	24	[11]
H1 low Q^2 HERA I dijets	2010	5	100	43.5	e^+p	301	no	22	16	[12]
H1 high Q^2 HERA II incl. jets	2014	150	15000	351	e^+p/e^-p	319	yes	24	24	[13]
H1 high Q^2 HERA II dijets	2014	150	15000	351	e^+p/e^-p	319	yes	24	24	[13]
H1 low Q^2 HERA II incl. jets	2016	5	80	290	e^+p/e^-p	319	yes	48	32	[14]
H1 low Q^2 HERA II dijets	2016	5	80	290	e^+p/e^-p	319	yes	48	32	[14]
ZEUS incl. jets HERA I	2002	125	10000	38.6	e^+p	301	no	30	30	[9]
ZEUS dijets HERA I and II	2010	125	20000	374	e^+p/e^-p	318	no	22	16	[10]

Table 1: The 8 data sets on jet production from H1 and ZEUS used for the HERAPDF2.0Jets NNLO (prel.) fits.

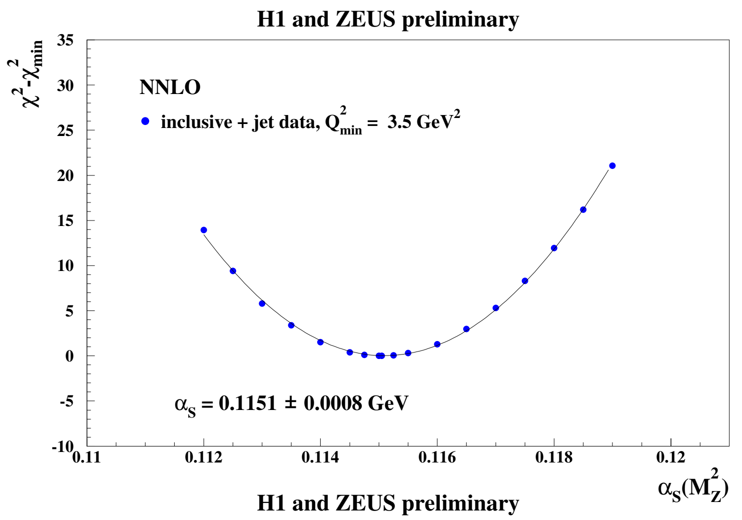

a)

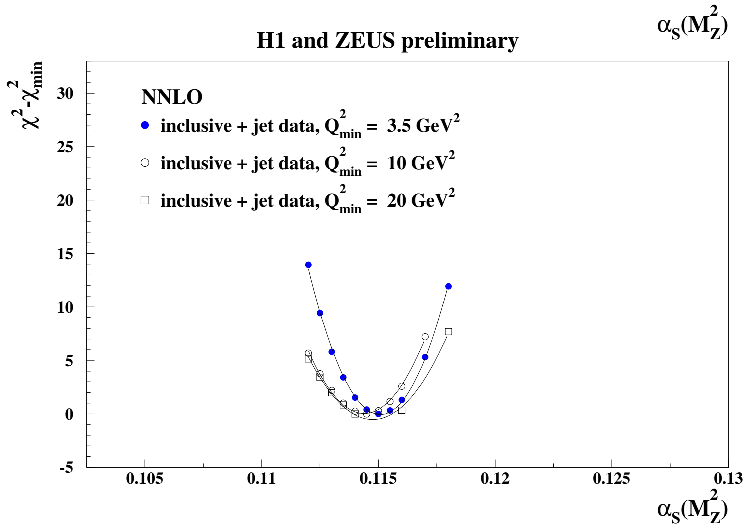

b)

Figure 1: $\Delta\chi^2 = \chi^2 - \chi^2_{\rm min}$ vs. $\alpha_s(M_Z^2)$ for HERAPDF2.0 NNLO (prel.) fits with fixed $\alpha_s(M_Z^2)$ with a) the standard Q^2_{min} of 3.5 GeV^2 b) with Q^2_{min} set to 10 GeV^2 for the inclusive data.

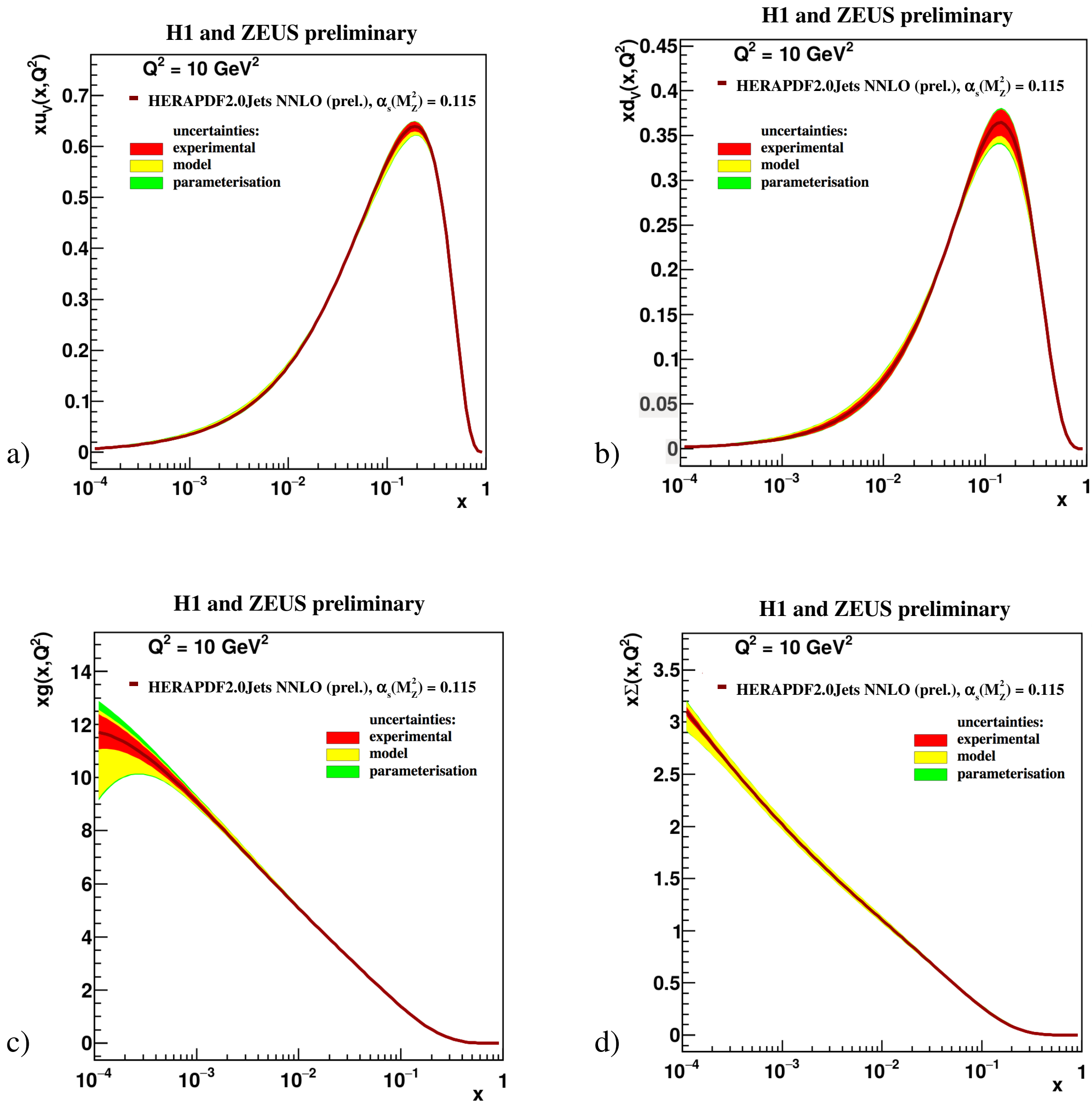

Figure 2: The parton distribution functions a) xu_v, b) xd_v, c) xg and d) $x\Sigma = 2x(\bar{U} + \bar{D})$ of HERAPDF2.0Jets NNLO (prel.) with $\alpha_s(M_Z^2)$ fixed to 0.115, the value determined in the NNLO fit with free $\alpha_s(M_Z^2)$ at the scale $Q^2 = 10\,\text{GeV}^2$. The uncertainties are given as differently shaded bands.

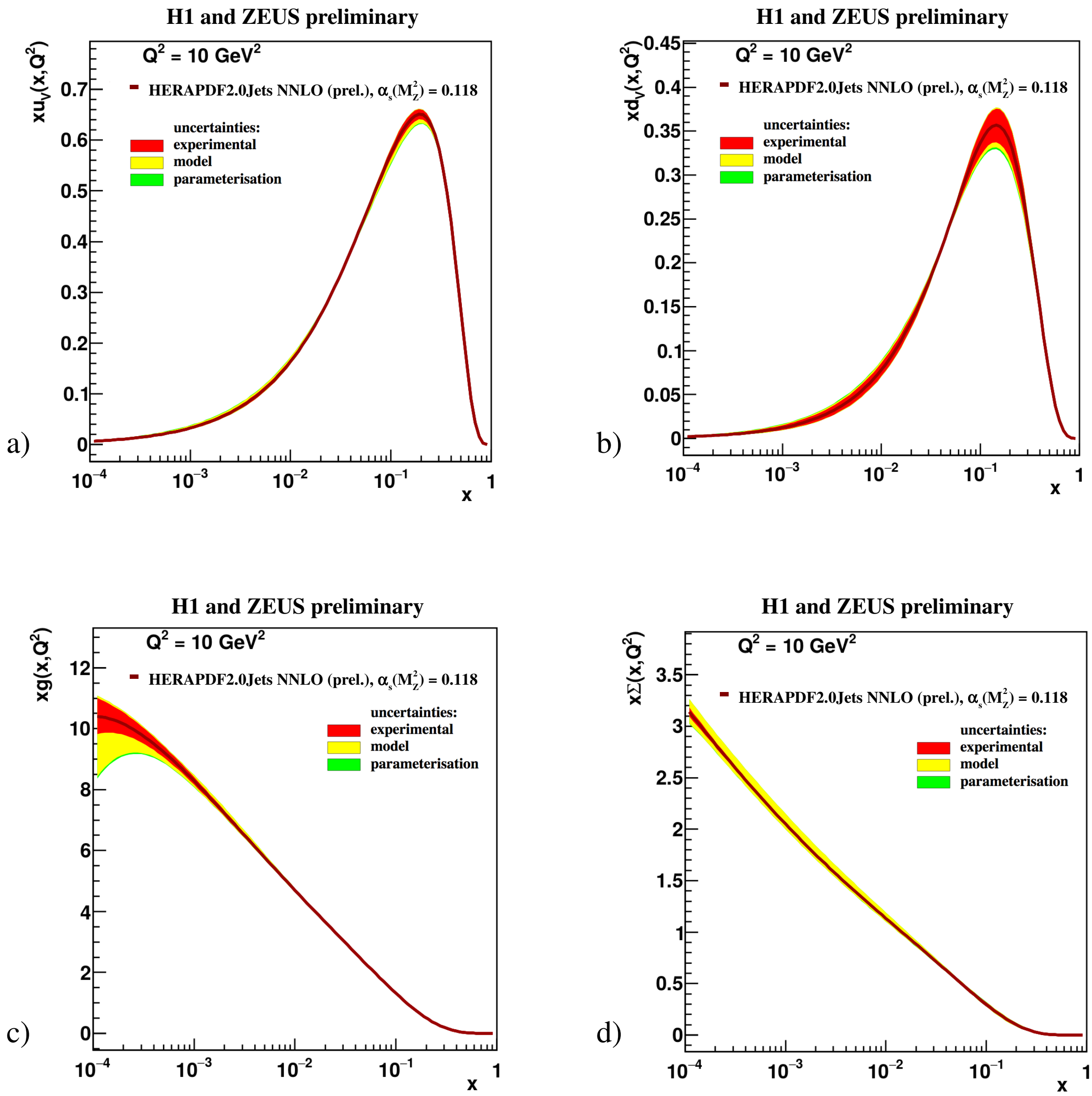

Figure 3: The parton distribution functions xu_v, xd_v, xg and $x\Sigma = 2x(\bar{U} + \bar{D})$ of HERAPDF2.0Jets NNLO (prel.) with $\alpha_s(M_Z^2)$ fixed to 0.118, the value determined in the HERAPDFJets NLO fit with free $\alpha_s(M_Z^2)$, at the scale $Q^2 = 10\,\mathrm{GeV}^2$. The uncertainties are given as differently shaded bands.

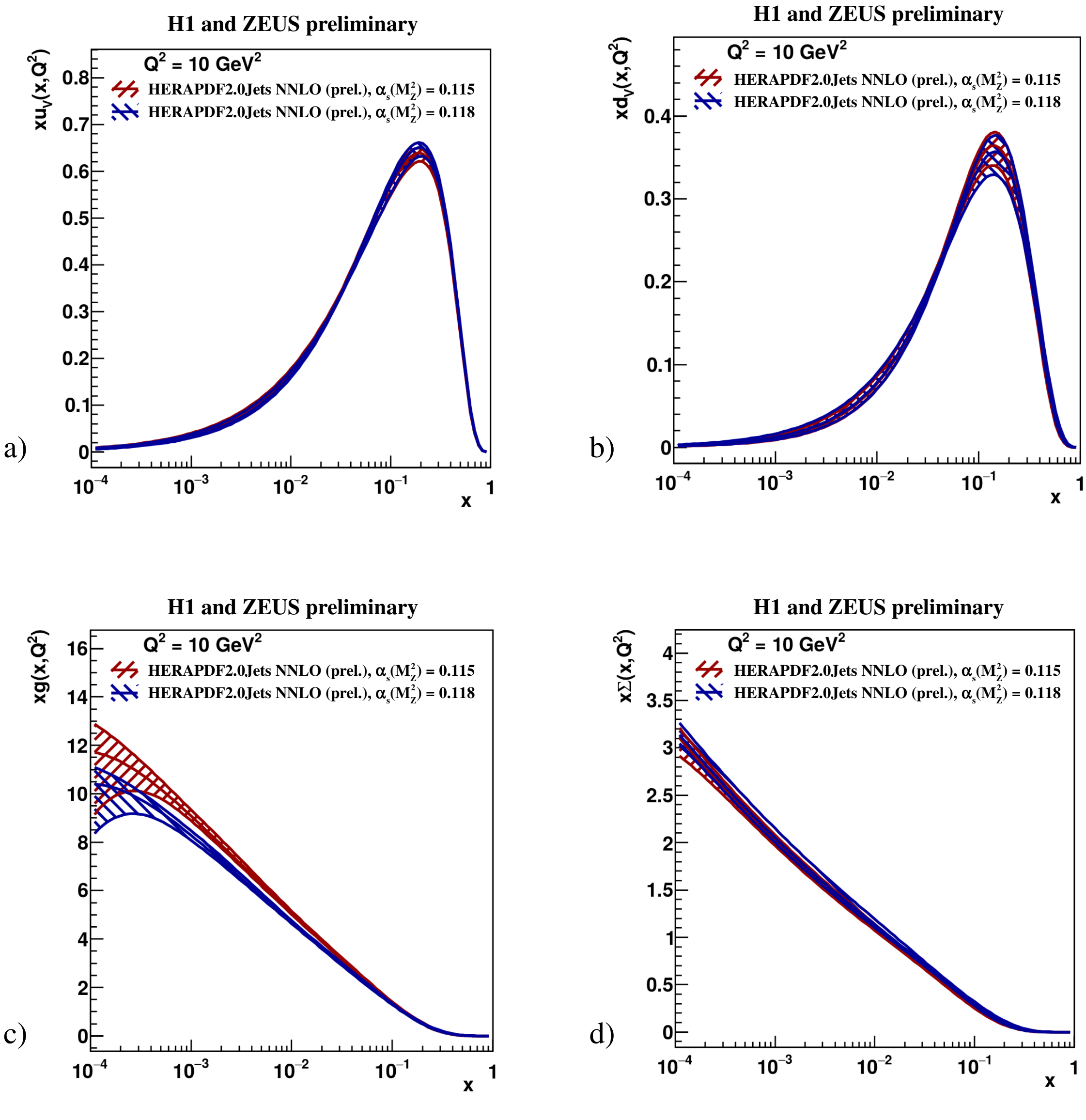

Figure 4: Comparison of the parton distribution functions a) xu_v, b) xd_v, c) xg and d) $x\Sigma = 2x(\bar{U} + \bar{D})$ of HERAPDF2.0Jets NNLO (prel.) with fixed $\alpha_s(M_Z^2) = 0.115$ and $\alpha_s(M_Z^2) = 0.118$ at the scale $Q^2 = 10\,\mathrm{GeV}^2$. The total uncertainties are shown as differently hatched bands.

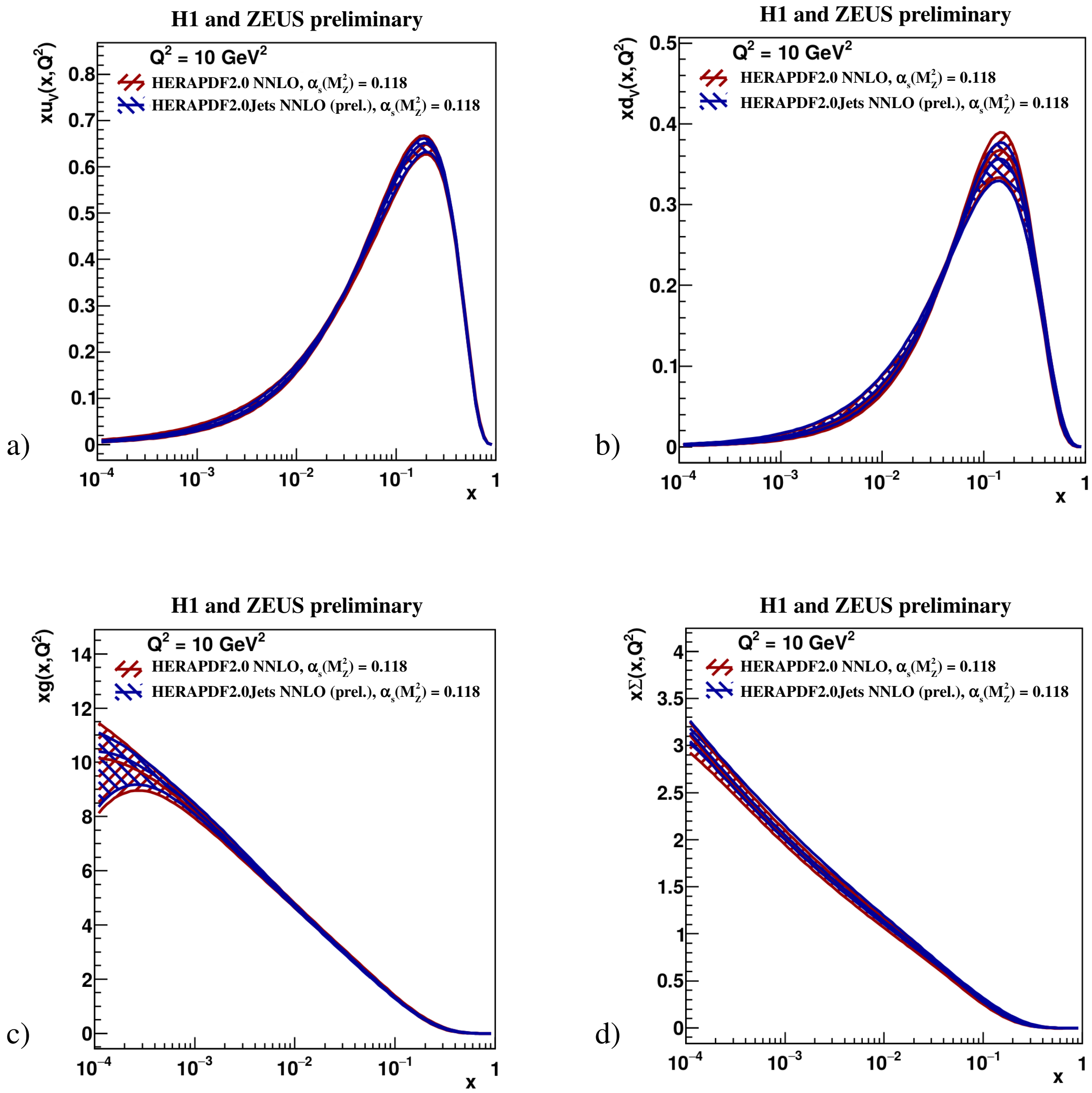

Figure 5: Comparison of the parton distribution functions a) xu_v, b) xd_v, c) xg and d) $x\Sigma = 2x(\bar{U} + \bar{D})$ of HERAPDF2.0Jets NNLO (prel.) and HERAPDF2.0 NNLO based on inclusive data only, both with fixed $\alpha_s(M_Z^2) = 0.118$, at the scale $Q^2 = 10\,\mathrm{GeV}^2$. The total uncertainties are shown as differently hatched bands.

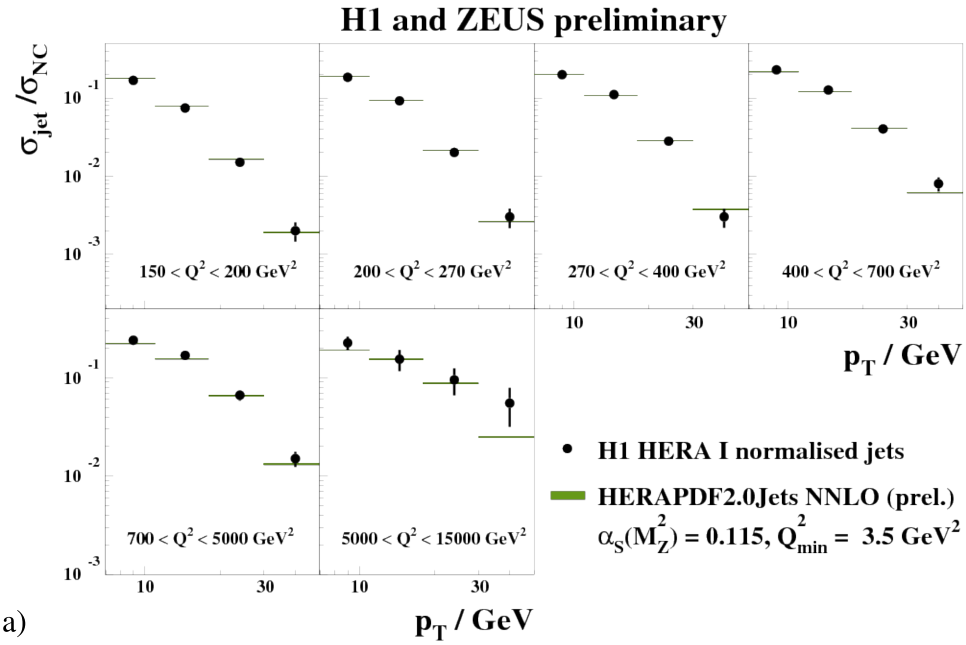

a)

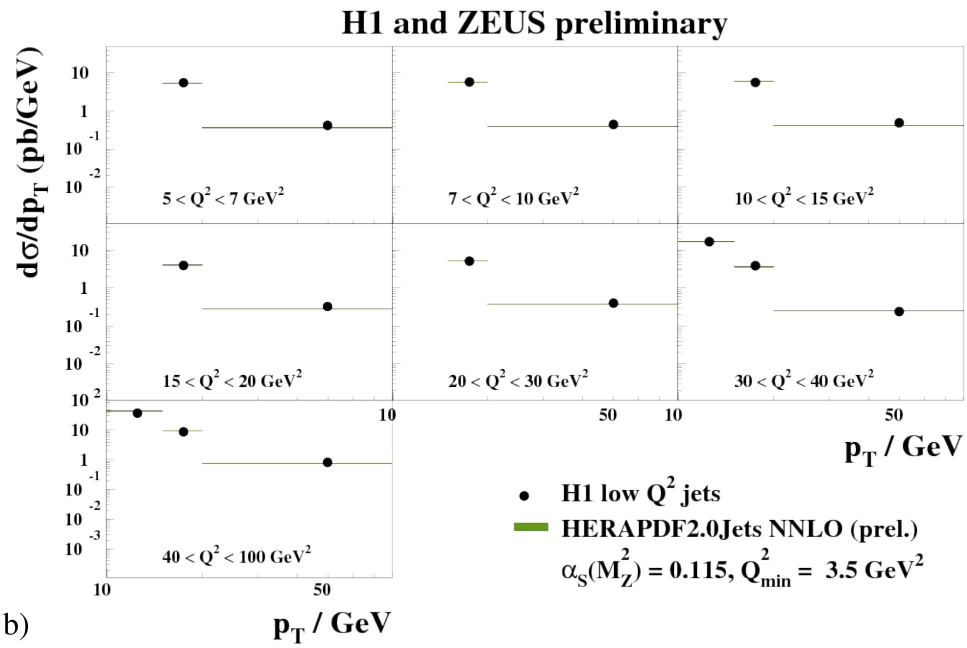

b)

Figure 6: a) Differential jet cross sections, $\mathrm{d}\sigma/\mathrm{d}p_T$, normalised to NC inclusive cross sections, in bins of Q^2 between 150 and 15000 GeV^2 as measured by H1. b) Differential jet cross sections, $\mathrm{d}\sigma/\mathrm{d}p_T$, in bins of Q^2 between 5 and 100 GeV^2 as measured by H1. Also shown are predictions from HERAPDF2.0Jets NNLO-prel. The bands represent the total uncertainties on the predictions excluding scale uncertainties.

a)

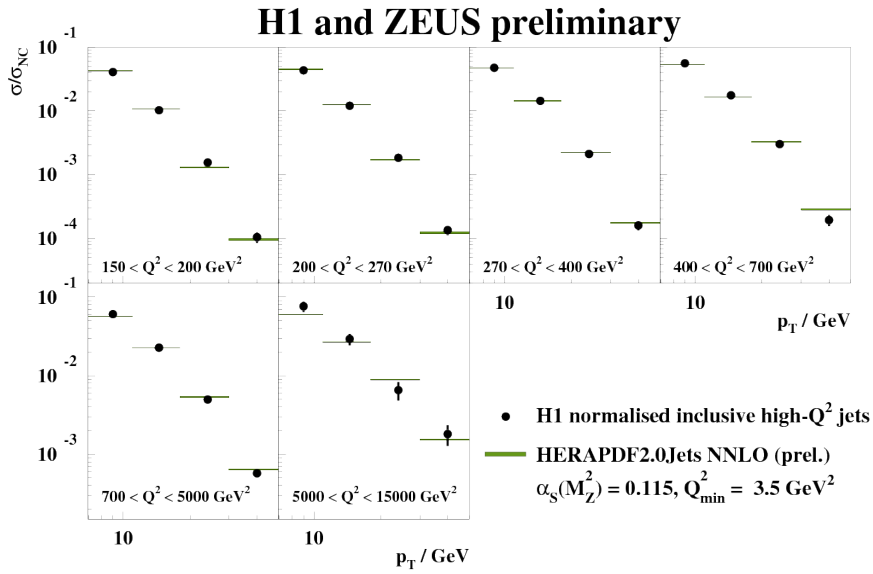

b)

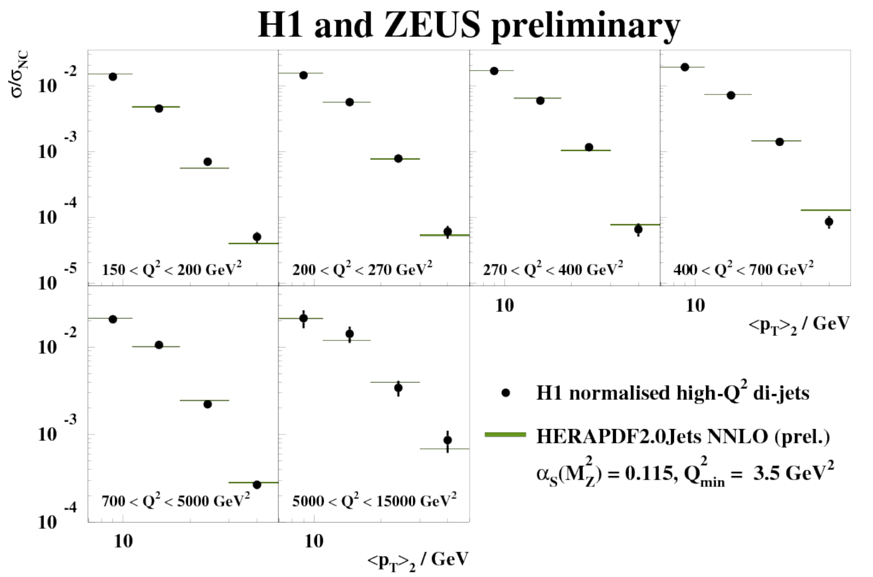

Figure 7: Differential normalised a) inclusive jet cross sections, $d\sigma/dp_T$, b) differential dijet cross-sections, $d\sigma/d\langle p_T\rangle_2$, in bins of Q^2 between 150 and 15000 GeV^2 as measured by H1. The variable $\langle p_T\rangle_2$ denote the average p_T of the two jets. All cross sections are normalised to NC inclusive cross sections. Also shown are predictions from HERAPDF2.0Jets NNLo-prel. The bands represent the total uncertainties on the predictions excluding scale uncertainties; they are mostly invisible.

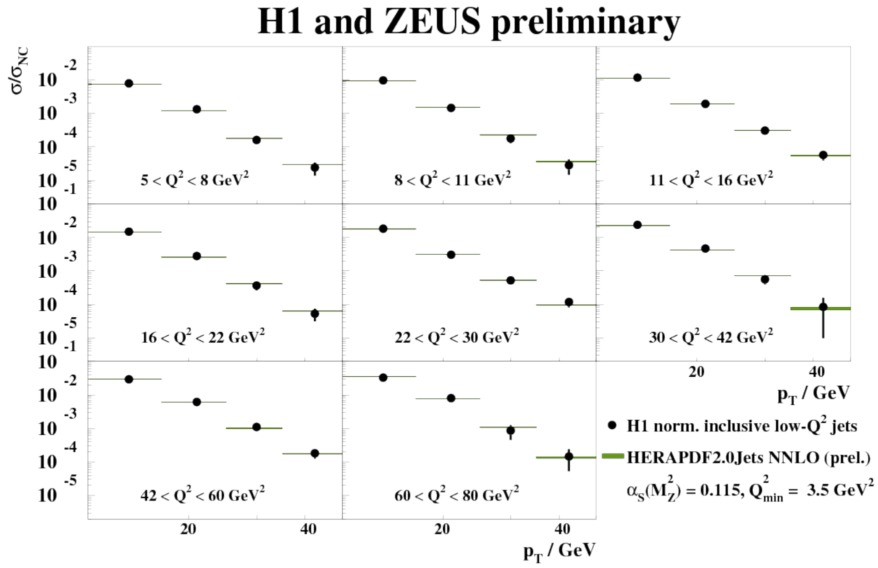

a)

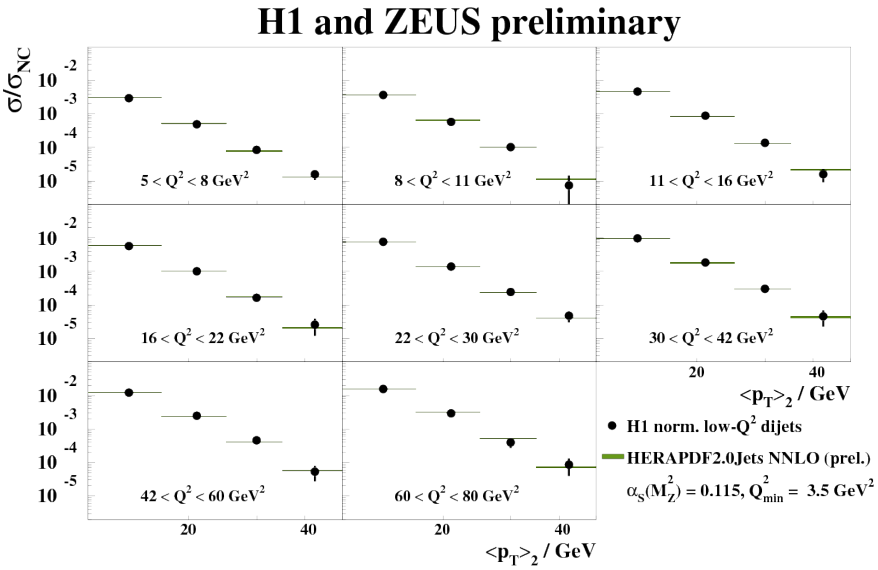

b)

Figure 8: Differential normalised a) inclusive jet cross sections, $d\sigma/dp_T$, b) differential dijet cross-sections, $d\sigma/d\langle p_T\rangle_2$, in bins of Q^2 between 5 and 80 GeV^2 as measured by H1. The variable $\langle p_T\rangle_2$ denote the average p_T of the two jets. All cross sections are normalised to NC inclusive cross sections. Also shown are predictions from HERAPDF2.0Jets NNLo (prel.) The bands represent the total uncertainties on the predictions excluding scale uncertainties; they are mostly invisible.

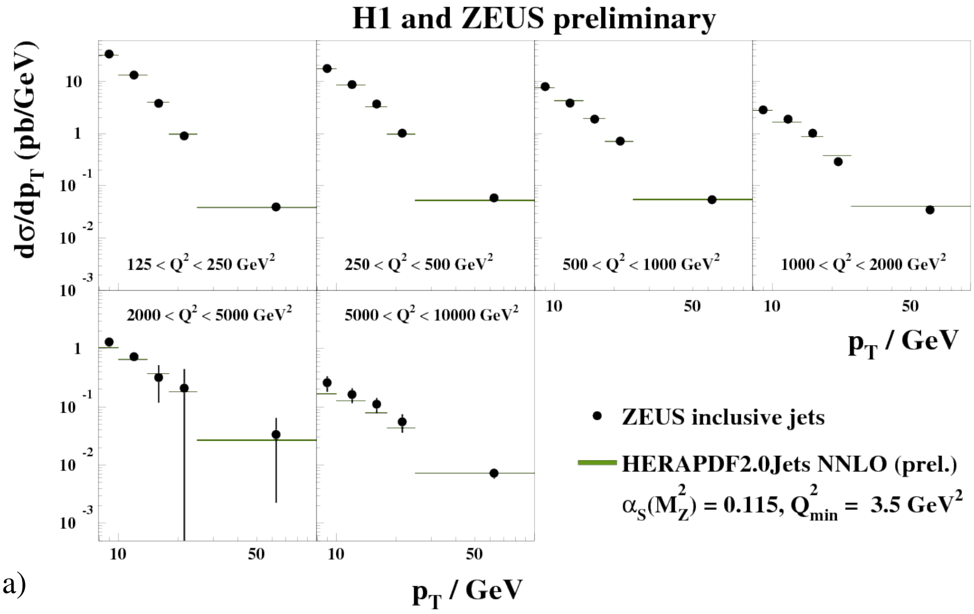

a)

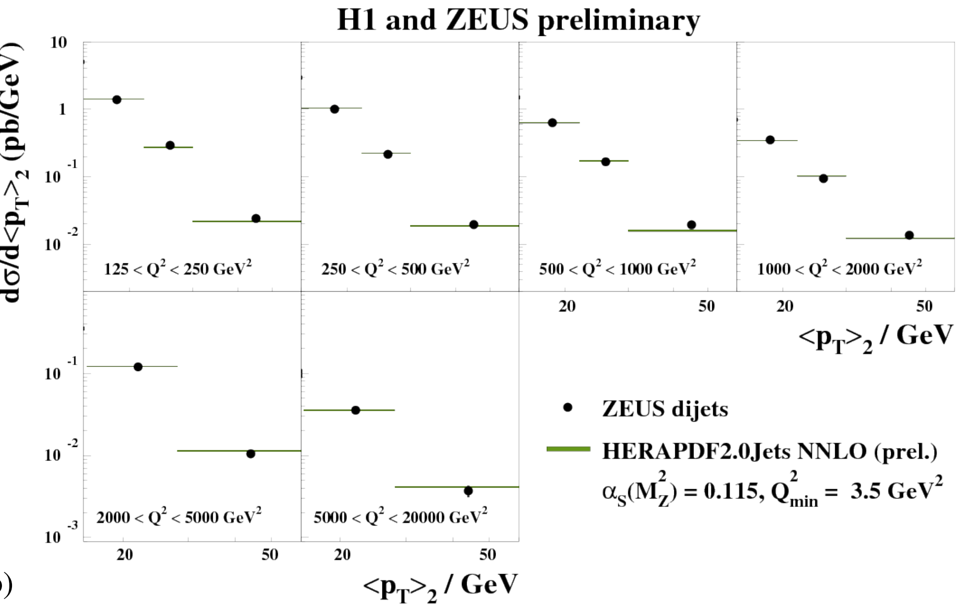

b)

Figure 9: a) Differential jet cross sections, $\mathrm{d}\sigma/\mathrm{d}p_T$, in bins of Q^2 between 125 and 10000 GeV^2 as measured by ZEUS. b) Differential dijet cross sections, $d\sigma/\mathrm{d}\langle p_T\rangle_2$, in bins of Q^2 between 125 and 20000 GeV^2 as measured by ZEUS. The variable $\langle p_T\rangle_2$ denotes the average p_T of the two jets. Also shown are predictions from HERAPDF2.0Jets NNLO-prel. The bands represent the total uncertainty on the predictions excluding scale uncertainties; they are mostly invisible.